Existence of an intrinsic glass transition in a silicon rubber: Hypersonic versus calorimetric properties

Jan K. Krüger, P. Mesquida, and J. Baller
Fachrichtung 10. 2 Experimentalphysik, Universität des Saarlandes, Gebäude 38, D-66123 Saarbrücken, Germany
(Received 9 March 1999)

Time-domain temperature-modulated differential scanning calorimetry and high-performance Brillouin spectroscopy have been used as experimental techniques in order to investigate the effect of the thermal glass transition on the specific heat as well as on the acoustic properties, quantities which are intimately related by thermodynamics, but measured at completely different frequencies. Using a siloxane as a model substance, we demonstrate the efficiency of hypersonic relaxations until thermal freezing of the material. Introducing the optoacoustic dispersion function as a sensitive measure for structural relaxations, we show that the high-frequency α relaxations are truncated by the thermal glass transition instead of dying out at much higher temperatures. Moreover, the extrapolated static compliance of the rubbery state goes to zero close to but below the thermal glass transition temperature T_g, indicating the existence of an acoustic instability which is reminiscent of the so-called Kauzmann paradox. [S0163-1829(99)07837-6]

INTRODUCTION

The difficulties in understanding the thermal glass transition are caused by extremely-low-frequency relaxation processes in the vicinity of the thermal glass transition temperature T_g. The main question in the understanding of the thermal glass transition is whether there exists at sufficiently slow cooling an underlying phase transition from the liquid to the ideal glassy state (transition hypothesis) or whether the thermal glass transition simply reflects the crossover of intrinsic relaxation times with typical time constraints of the experimental technique used (kinetic hypothesis).[1–7]

Recent experimental progress in the field of high-resolution Brillouin spectroscopy (BS) on polyvinylacetate[10] (PVAC) and on an epoxy[11,12] (EPON) polymer have supported the idea of such an underlying transition which is believed to take place from the equilibrium liquid phase into a nonergodic glass phase. Among other results this conclusion was drawn from a discontinuity in the longitudinal-mode Grüneisen parameter at T_g as well as from the temperature behavior of the structural glass relaxation process (α relaxation) which showed a clear cutoff just below T_g.[8]

In a glass-forming liquid the static longitudinal stiffness modul c_{11} behaves ''steplike'' at T_g, whereas the static shear stiffness c_{44} is zero above T_g and nonzero below T_g. At hypersonic frequencies c_{44} as well as c_{11} shows a kinklike behavior thus reflecting the fact that above but close to T_g the elastic constants are (almost) clamped. In other words, slightly above T_g, hypersonic measurements are believed to be made in the slow-motion regime in relation to the structural α-relaxation process. In the glassy state hypersonic data usually reflect static second- and third-order elastic properties[10] belonging to the solidlike properties of glasses. Consequently, acoustic-mode Grüneisen parameters correspond to those of solids.[9,10] Provided that the elastic properties are dynamically clamped properties, the kink in the high-frequency elastic properties versus temperature relation should be attributed to an intrinsic change of the acoustic anharmonicity at T_g.

In the present paper we apply the optoacoustic dispersion function (OADF) for the longitudinal polarized acoustic mode as a particular sensitive measure for static as well as for dynamic hypersonic properties. We use this technique in order to investigate the thermal glass transition of a partially crystallizing and subsequently freezing silicon rubber. We will show that the unusual temperature behavior of the OADF around the thermal glass transition of this siloxane yields further support for the transition hypothesis, demonstrating that the α-relaxation process as measured at hypersonic frequencies may extend until T_g, but is truncated by the thermal glass transition. Moreover, the transition hypothesis will be supported by supplying evidence for an acoustic analog to the so-called ''Kauzmann paradox.''

EXPERIMENT

The siloxane under study, SilGel 604, is a standard silicon rubber of the RTV-2 group produced by Wacker Chemie, München. SilGel 604 is a highly transparent silicon rubber which is made by addition vulcanization from the two parent products. The material shows no measurable shrinkage after the vulcanization process.

Figure 1 gives the schematics of the network-forming molecule. The chemical constitution of the organic group R was not available from Wacker Chemie. Although the vulcanized SilGel 604 does still crystallize, because of the chemical network formed during the vulcanization process, this crystallization is never complete, which, on the other hand, implies that there exists a maximum crystallinity which is well below 100%. The remaining amorphous matrix necessarily undergoes a thermal glass transition and shows a glass transition temperature $T_g = 148$ K, which is well below the equilibrium melting temperature $T_m = 235.15$ K.

The SilGel 604 has the special property of almost nonsticking to its surroundings. This ''low-adhesion'' property turned out especially useful for the investigation of the thermal glass transition of this material because it reduces the amount of thermoelastic stresses when cooling the sample

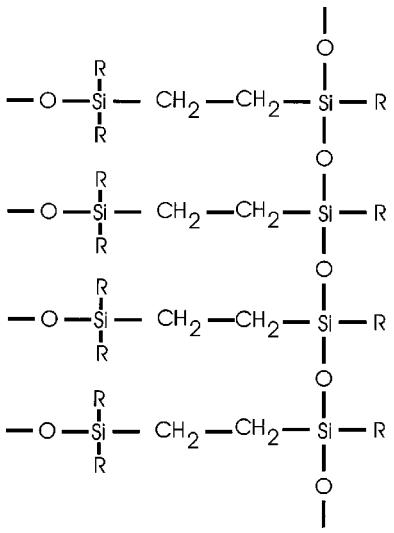

FIG. 1. Schematics of the network of SilGel 604: addition vulcanized silicon rubber. *R*: organic substituent.

within a container of a different thermal expansion coefficient. However, as will be shown below, even in this material undesirable stresses may develop under certain circumstances and consequently strongly modify the glass transition behavior of the material.

The high-performance Brillouin technique (BS) presented in this paper has been described elsewhere.[11] For the BS measurements a filmlike sample of about 200 μm thickness and about 10 mm diameter was vulcanized between two glass slides. Thus the sample surfaces had a high optical quality in the entire temperature range of the investigations. Any bending of the sample during the course of the experiments was avoided by means of the two glass slides. After having finished the BS measurements, the glass slides were removed and the refractive index of the sample was determined with an Abbé refractometer, yielding at 300 K a value of $n_{514.5}=1.404$.

In order to obtain the required long-time stability, the temperature of the spectrometer including the spectrometer control was stabilized to better than 0.1 K. Moreover, the data collection procedure and the evaluation of the data have been completely automated, yielding immediately the final Brillouin data after each measurement. The spectrometer is able to run completely stable without the need of any human interaction over many months.

For investigations as a function of temperature, the sample was positioned within a self-made top-loading thermostat. The temperature control was maintained with a PID controller (ITC-4, Oxford Instruments) using a rhodium-iron resistance. Using simultaneously the scattering geometries 90*A* (outer scattering angle $\theta_o=90°$) and 18 (back scattering) [Fig. 2(a)], we get the hypersonic frequencies f^{90A} and f^{18} for two different wave vectors $\mathbf{q}^{90A}$ and $\mathbf{q}^{18}$ from the same scattering volume as a function of temperature.

The measurements performed at ambient temperature as a function of the acoustic wave vector $\mathbf{q}$ ($\mathbf{q}^{\Theta A}$ scan) were made using a goniometer which has been built in the laboratory especially for this purpose. In order to make $\mathbf{q}^{\Theta A}$-scan measurements, the filmlike sample is spread on an aluminum mirror [MR in Fig. 2(b)]. As is also shown in Fig. 2(b), the $\mathbf{q}^{\Theta A}$ scan performed on an isotropic sample simultaneously yields the phonon frequencies f^{18} and $f(\mathbf{q}^{\Theta A})=f^{\Theta A}$. It is interesting to note that the phonon wave vector $\mathbf{q}^{\Theta A}$ is automatically fixed in the film plane of the sample.

In order to control the influence of local heating of the sample by the laser beam, we made Brillouin measurements as a function of laser power. The final Brillouin measurements were performed with an incident laser power of about 30 mW.

The time-domain temperature-modulated differential scanning calorimetry (TMDSC) measurements were performed with a significantly modified commercial instrument. The details of our TMDCS setup and the measurement technique have been described in more detail elsewhere.[12]

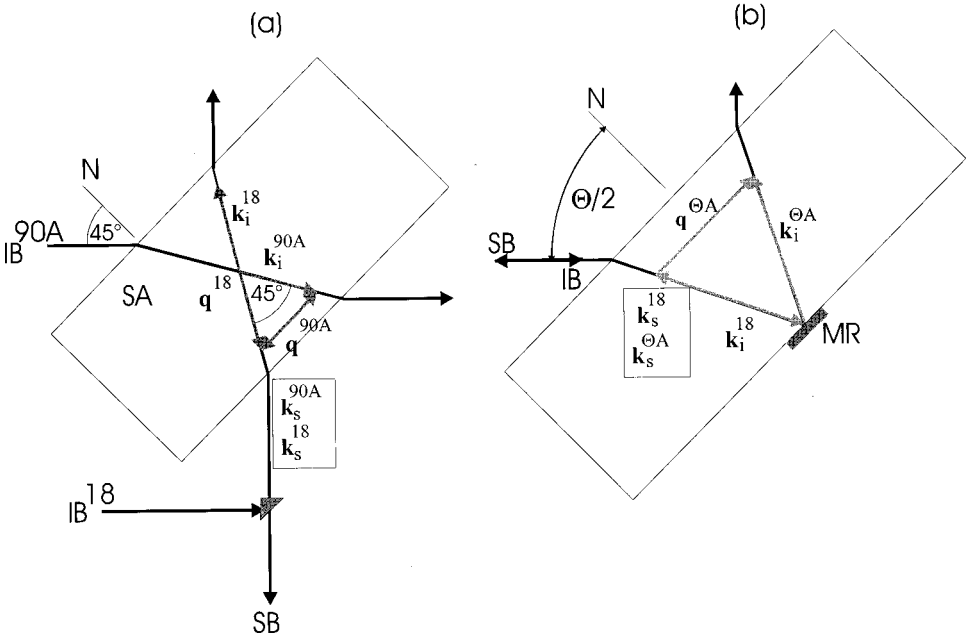

FIG. 2. (a) 90*A*, backscattering and (b) θA scattering geometries. IB: incident beam. SB: scattered beam. $\mathbf{k}_i^{90A}$, $\mathbf{k}_i^{18}$, $\mathbf{k}_i^{\theta A}$, $\mathbf{k}_s^{90A}$, $\mathbf{k}_s^{18}$, and $\mathbf{k}_s^{\theta A}$: wave vectors of the incident laser beam and of the scattered light, respectively. $\mathbf{q}^{90A}$, $\mathbf{q}^{18}$, and $\mathbf{q}^{\theta A}$: phonon wave vectors in 90*A*, backscattering, and θA geometry, respectively. SA: sample. MR: mirror.

RESULTS AND DISCUSSION

Using BS as an experimental probe for the static and dynamic glass transition, it is obvious that the Brillouin frequency f detects static as well as dynamic elastic properties, whereas the hypersonic attenuation Γ is sensitive only for dynamic processes. That is the reason why usually Γ instead of f is used to characterize hypersonic relaxations. However, the measurement accuracy for the hypersonic attenuation Γ is by about a factor of 10 smaller than that of the sound frequency f. We therefore were interested in a quantity based on the sound frequency f which clearly separates static and dynamic contributions to the elastic properties on the one hand, but which, on the other hand, takes profit of the fact that it is easier to perform precise measurements of the sound frequency f.

The optoacoustic dispersion function $D^{X,\Theta A}$ turns out to have these desired properties:[13]

$$D^{X,\Theta A}(T)=n(T)\sqrt{\frac{c'^{X}(T)}{c'^{\Theta A}(T)}}. \tag{1}$$

In Eq. (1), c' refers to the real part of the complex elastic stiffness constant $c^*=c'-ic''$, X refers to a phonon wave vector $\mathbf{q}^X$ depending on the refractive index n of the sample, which is assumed to be isotropic, ΘA refers to the phonon wave vector $\mathbf{q}^{\theta A}$, which is symmetry equivalent to $\mathbf{q}^X$, and T is the temperature of the sample. Furthermore, we admit that the sample shows only moderate attenuation ($c''\ll c'$), which yields

$$v(p,\mathbf{q})=\frac{2\pi f(p,\mathbf{q})}{|\mathbf{q}|} \tag{2}$$

and $c'(p,\mathbf{q})=\rho v^2(p,\mathbf{q})$.

If there is no acoustic dispersion ($c'^{X}=c'^{\Theta A}$), Eq. (1) yields directly the refractive index n of the sample. Using the q-scan method shown in Fig. 2(b), we have $X=18$ (backscattering) and Eq. (1) may be written as

$$D^{18,\Theta A}(T)=\sin\left(\frac{\Theta A}{2}\right)\frac{f^{18}(T)}{f^{\Theta A}(T)}\geqslant n, \tag{3}$$

where we have used

$$q^{18}=\frac{4\pi n}{\lambda_0}\quad\text{and}\quad q^{\Theta A}=\frac{4\pi\sin(\Theta A/2)}{\lambda_0}, \tag{4}$$

where λ_0 is the vacuum wavelength of the laser.

It is worth noting that in the acoustic dispersion-free case Eq. (3) yields the refractive index from the simultaneously measured hypersonic frequencies f^{18} and $f^{\Theta A}$. In that case we have direct access to changes of the refractive index or the establishment of birefringence as a function of temperature, which both may develop in the course of phase transitions.

Figure 3 shows a $q^{\Theta A}$-scan measurement of SilGel 604 at 300 K, covering an acoustic wavelength $\Lambda^{\Theta A}=\lambda_0/(2\sin(\theta/2))$ from 0.26 to 1 μm. As expected, as a function of $\sin(\Theta A/2)\propto q^{\Theta A}$ the frequency of the Brillouin lines obtained by backscattering, f^{18}, is quite a horizontal line, whereas the frequency $f^{\Theta A}$ is a straight line where the slope

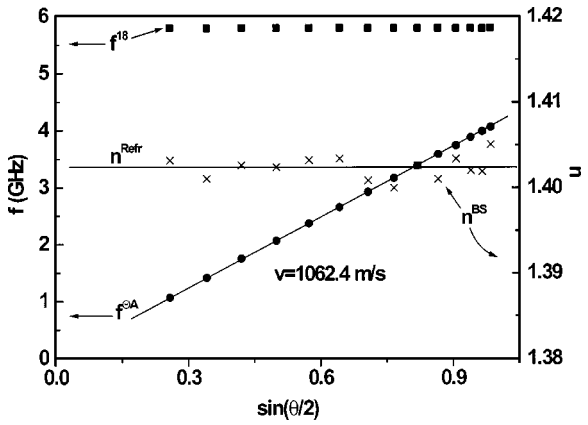

FIG. 3. SilGel 604: hypersonic frequencies f^{18} and $f^{\Theta A}$ obtained by backscattering and by θA scattering, respectively. n: refractive index.

of this curve gives the sound velocity intersecting zero for $\mathbf{q}^{\Theta A}=0$. This linear dispersion behavior demonstrates that at ambient temperature relaxation effects are negligible for the acoustic wave vectors involved. Moreover, the fact that $f^{\Theta A}$ as a function of $\sin(\Theta A/2)$ goes through zero implies that the related sound velocity at this temperature was measured in the fast-motion regime. Consequently, $D^{18,\Theta A}=n$ holds and n can be calculated using Eq. (3). Obviously, this behavior has to change by crossing the α process on approaching the thermal glass transition. Within the hypersonic relaxation regime the $D^{18,\Theta A}(T)$ function has to deviate from the $n(T)$ function.[10] In order to elucidate the hypersonic relaxation behavior around the dynamic and static glass transitions, we therefore have performed BS measurements as a function of temperature using the scattering arrangement illustrated in Fig. 2(a).

The frequencies f^{90A} and f^{18} shown in Fig. 4 were measured on cooling the sample from 300 K down to about 80 K. From these frequencies we have derived the related OADF $D^{18,90A}(T)$. Both hypersonic frequency curves show three significant anomalies at the temperatures $T_{\text{cryst}}=207$ K, $T_g=148$ K, and $T_r=119$ K. Here T_{cryst} indicates the onset of a partially crystallization after undercooling the sample and T_g reflects the thermal glass transition on slow cooling.

The discontinuity within the sound frequency curves at T_r demonstrates a usual problem related to investigations of

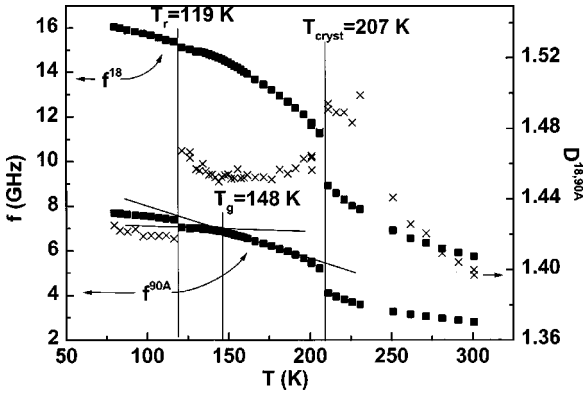

FIG. 4. Hypersonic frequencies f^{90A} and f^{18} of SilGel 604 as a function of temperature. $D^{18,90A}$: optoacoustic dispersion function. The measurements were performed on cooling.

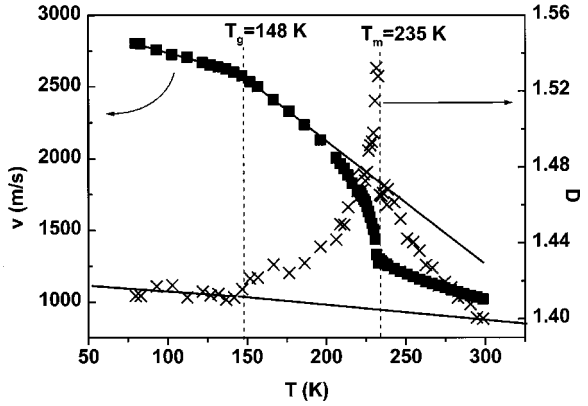

FIG. 5. Sound velocity v and dispersion function D vs temperature. The measurements were performed on heating.

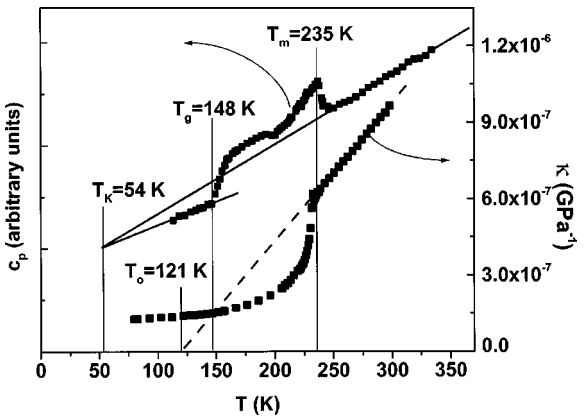

FIG. 6. Specific heat capacity c_p and elastic compliance (compressibility) κ of SilGel 604. The measurements were performed on heating.

transitions from the fluid (rubber) to the glassy state: because of the fluidity (flexibility) at temperatures well above T_g, a glass-forming liquid (rubber) has to be held within a container. As was mentioned above, in our case the sample was vulcanized between two glass slides. Usually, the sample then sticks to the walls of the container. Due to the different thermal expansion coefficients of the sample and container, material significant internal stresses may be built up. If these stresses become large enough, the sample may crack, the container may crack, or as in our case just the contact surface between sample and container changes. Obviously, the released internal stresses cause increased longitudinal sound frequencies below T_r. In our special case of an only slightly sticking rubber sample, the sudden mechanical relaxation of the sample happens 29 K below T_g. Usually, it is hard to predict when a sample mechanically relaxes or whether it relaxes at all in the temperature interval under consideration. As soon as the sample is hold in a container, the sticking effect generally makes the interpretation of investigations of the liquid-glass transition unreliable. Only if the sample has already obviously mechanically relaxed can reliable temperature-dependent measurements be done.

The OADF $D^{18,90A}(T)$ displayed in Fig. 4 shows at room temperature the expected value of the refractive index n but increases strongly on approaching the crystallization process. Because the $D^{18,90A}(T)$ function decreases below T_{cryst} on approaching T_g, it seems that hypersonic relaxation processes are active between T_g and 300 K. In addition, the refractive index may have changed by the crystallization process. However, crystallization would not explain the decrease of $D^{18,90A}(T)$ between T_{cryst} and T_g. Between T_g and T_r the quantity $D^{18,90A}(T)$ increases rather strongly, which is indicative of the onset of stress birefringence. Only after the sample mechanically had relaxed at T_r did the $D^{18,90A}(T)$ function approach the expected refraction behavior of the stress-free glass.

Measuring the once mechanically relaxed sample on heating, we obtained the results given in Fig. 5. As expected, the mechanically relaxed sample shows only two acoustic anomalies: the kink within the longitudinal sound velocity curve at T_g and a further kink at the end of the melt transition. Within the margin of error the sound velocity curve behaves continuously throughout the glass transition as well as at the melt transition. The $D^{18,90A}(T)$ function shows in the low-temperature regime ($T<T_g$) a decrease with increasing temperature, as expected for the refractive index n. Immediately above T_g the $D^{18,90A}(T)$ function increases, indicating the immediate onset of the hypersonic α-relaxation process. This behavior is in contrast to that found in linear polymers such as polymethyl methacrylate (PMMA), polystyrene (PS), and PVAC,[8] but resembles that of an epoxy (EPON).[9] For SilGel 604 we therefore come to the same conclusions which we discussed recently for EPON.[9] It seems that the slowing down of the α process does not drive the thermal glass transition, but the opposite case seems to be true. It looks like that at least the high-frequency α relaxations are truncated by the thermal glass transition at T_g. In this sense the ideal glass transition seems not to reflect the crossover of intrinsic and experimental time scales, although this slowing down influences the experimental results.

In order to give further support to the existence of an intrinsic thermal glass transition, we have tried to find hints of the existence of a potential acoustic instability below the operative thermal glass transition in the sense of an analog to the thermal Kauzmann paradox (Fig. 6). This attempt seems to be reasonable, since the glass transition transforms a liquid state into a solid state and consequently a hypothetical order parameter is expected to couple to the elastic compliance.

The elastic compliance (compressibility) κ can immediately be obtained from our f^{90A} data:

$$\kappa=\frac{3}{3c_{11}-4c_{44}}=\frac{3}{\rho(3v_L^2-4v_T^2)}=\frac{3}{\rho}\left(\frac{q^{90A}}{3f_L^{90A}-4f_T^{90A}}\right)^2. \tag{5}$$

For the fast-motion regime ($c_{44}=0$), the following simple relation holds:

$$\kappa=\frac{1}{\rho}\left(\frac{q^{90A}}{f_L^{90A}}\right)^2. \tag{6}$$

Here ρ is the mass density (set equal to 1000 kg/m^3), v_L and v_T are the static longitudinal and static transverse sound velocities, respectively, and f_L^{90A} and f_T^{90A} are the related sound frequencies. The κ representation shows three prominent features, yielding the temperatures $T_0=121\,\mathrm{K}$, $T_i=T_g$

$=148$ K, and $T_m=235$ K. The end of the melting process is indicated by a marked kink within the $\kappa(T)$ curve, which above T_m behaves linearly with increasing temperature. The extrapolation of this linear compliance branch to lower temperatures yields the temperature $T_i=T_g$, where the extrapolated static compressibility curve intersects the measured compressibility curve. At the temperature T_0 the extrapolated compressibility curve definitely becomes zero. At T_0 $(=T_g-27\,\mathrm{K})$ the liquid would become incompressible, which is not believed to be a realistic state of condensed matter. We therefore believe that T_0 defines a lower limit for the ideal glass transition temperature T_{gs}. In reality, $T_{gs}>T_0$ should hold. In this context T_i seems to be an upper limit for T_{gs}.

The temperature dependence of the acoustic data may be compared with those of the specific heat capacity $c_p(T)$ (Fig. 6) as measured with time-domain TMDSC.[12] The intersection temperature T_i perfectly coincides with the thermal glass transition at T_g, defining the onset of excess specific heat.

As a result of our analysis of the dynamic and static acoustic behavior around the thermal glass transition, we believe we have shown further evidence for the existence of an ideal glass transition.

ACKNOWLEDGMENT

We gratefully acknowledge the support by the Deutsdie Forschungsgemeinschaft.

[1] J. Jäckle, Rep. Prog. Phys. **49**, 171 (1986); J. Phys.: Condens. Matter **1**, 267 (1989).
[2] K. Binder, Ber. Bunsenges. Phys. Chem. **100**, 1381 (1996).
[3] E. Donth, *Relaxation and Thermodynamics in Polymers, Glass Transition* (Akademie-Verlag, Berlin, 1992).
[4] J. H. Gibbs and E. A. DiMarzio, J. Chem. Phys. **28**, 373 (1958); G. Gee, Contemp. Phys. **11**, 313 (1970).
[5] W. Götze and L. Sjögren, Rep. Prog. Phys. **55**, 241 (1992).
[6] J. Kovacs, J. J. Aklonis, J. M. Hutchinson, and A. R. Ramos, J. Polym. Sci., Polym. Phys. Ed. **17**, 1097 (1979).
[7] J. K. Krüger, K.-P. Bohn, and R. Jiménez, Condens. Matter News **5**, 10 (1996).
[8] J. K. Krüger, K.-P. Bohn, and J. Schreiber, Phys. Rev. B **54**, 15 767 (1996).
[9] K.-P. Bohn and J. K. Krüger, in *Structure and Properties of Glassy Polymers*, ACS Symposium Series Vol. 710, edited by M. R. Tant and A. J. Hill (American Chemical Society, Washington, DC, 1998), Chap. 5.
[10] J. K. Krüger, A. Marx, and L. Peetz, Ferroelectrics **26**, 753 (1980).
[11] J. K. Krüger, in *Optical Techniques to Characterize Polymer Systems*, edited by H. Bässler (Elsevier, Amsterdam, 1989).
[12] K.-P. Bohn, A. Prahm, J. Petersson, and J. K. Krüger, Thermochim. Acta **304/305**, 283 (1997).
[13] J. K. Krüger, J. Embs, J. Brierley, and R. Jimenez; J. Phys. D **31**, 1913 (1998).